

**Effect of symmetry on the resistive characteristics of proximity coupled metallic multilayers**V. N. Kushnir,<sup>1</sup> S. L. Prischepa,<sup>1</sup> M. L. Della Rocca,<sup>2</sup> M. Salvato,<sup>2</sup> and C. Attanasio<sup>2</sup><sup>1</sup>*State University of Informatics and RadioElectronics, P. Brovka 6, Minsk 220013, Belarus*<sup>2</sup>*Dipartimento di Fisica "E.R. Caianiello" and INFM, Università degli Studi di Salerno, I-84081 Baronissi (SA), Italy*

(Received 2 July 2003; published 31 December 2003)

The influence of finite dimensions of metallic multilayers on the superconducting phase nucleation and vortex mobility is studied. Resistive characteristics are sensitive to the geometrical symmetry of the samples. For multilayers with the symmetry plane in the center of superconducting layer the resistive transitions are widely spread for temperatures above the temperature of two- to three-dimensional crossover with respect to the samples with the symmetry plane in the center of the normal layer. Applying the Ginzburg-Landau theory, we correctly found the upper critical magnetic fields and explained the observed broadening by considering the common action of the Lorentz and pinning forces on the nascent vortex lattice.

DOI: 10.1103/PhysRevB.68.212505

PACS number(s): 74.78.Fk, 74.20.De, 74.45.+c

During the last decades, the study of superconducting properties and vortex matter in different kinds of multilayers has attracted an increasing interest.<sup>1</sup> The superconductivity in layered systems is closely related to the spatial behavior of the order parameter, which allows us a better understanding of the nucleation of superconducting phase in multilayers. As a result one can extract information about both the superconducting phase transition and the pinning mechanisms of the vortex medium in the presence of periodicity, which are still open issues.<sup>2-7</sup>

An alternating sequence of normal metal and superconductor layers (N/S) creates a system whose properties could be well described within the existing microscopic and phenomenological theories. The background for the microscopic theoretical investigation of infinite metallic multilayers in the vicinity of the upper critical magnetic field  $H_{c2}$ , has been given by Takahashi and Tachiki (TT).<sup>2</sup> The TT theory is for the case of infinite superlattices, and this approach yields different difficulties, especially when trying to fit experimental data for the parallel critical magnetic field  $H_{c2\parallel}(T)$ .<sup>3</sup> Recently this problem was resolved by Ciuhu and Lodder.<sup>8,9</sup> They analyzed the case of finite N/S samples, where surface superconductivity<sup>10</sup> and the finite boundary resistivity of the N/S interfaces<sup>11</sup> can significantly influence the  $H$ - $T$  plot. Numerical detailed study of the effect of finite dimensions of N/S multilayers on their thermodynamic properties reveals that surface superconductivity indeed appears, depending on the thickness of the outer N layers  $d_N^{\text{out}}$ .<sup>8</sup> As for isotropic homogeneous superconductors, when  $d_N^{\text{out}}$  are thick enough with respect to the coherence length  $\xi$  (in Ref. 8 the calculations were done for  $d_N^{\text{out}} = 350 \text{ \AA}$ ), bulk rather than surface superconductivity occurs in multilayer. In this case an essential improvement in fitting the  $H_{c2}(T)$  curves was obtained by taking into account the finite boundary resistivity of the N/S interfaces.<sup>9</sup> Nevertheless, the problem of the influence of the surface superconductivity on the temperature dependence of the parallel upper critical magnetic field still remains when  $d_N^{\text{out}} \leq \xi$ .<sup>10</sup> At this point a phenomenological extension of the microscopic theory should be applied. The macroscopic Ginzburg-Landau (GL) theory<sup>12</sup> is indeed widely used for studying the behavior of superconductors in a magnetic

field. In the general case it is impossible to find the exact solution of the GL equations analytically, and numerical computations are used or various limiting cases are studied. In particular, the continuous GL model<sup>13</sup> is convenient for a description of the complex order parameter  $\Psi$  and  $H_{c2}$  of layered superconductors.

In this paper we report the results of the effect of the finiteness of the N/S multilayers with a variable number of bilayers  $N_b$  and, consequently, with a variable symmetry, on the resistive characteristics in parallel magnetic field. All the experiments have been performed on proximity coupled Cu/Nb multilayers, which is a very well studied system due to the works of Schuller and co-workers.<sup>11,14</sup> The variable number of Cu/Nb bilayers, plus a covering Cu layer at the top of the structures, control the finite thickness of the samples and their actual symmetry. In fact, for odd  $N_b$  the symmetry plane is located inside the Superconducting layer (S-type samples), while for even  $N_b$  the symmetry plane is situated inside the normal metal layer (N-type samples). We show that for N-type samples the resistive transitions  $\rho(T)$  are always sharp curves revealing the resistive rapid fall down to zero in the whole magnetic field range. For S-type samples in the absence of the applied magnetic field the  $\rho(T)$  curves are always sharp. But in parallel field in a certain temperature range  $0.6T_c < T < 0.9T_c$  the  $\rho(T, H)$  transitions are broadened. Finally, at  $T < 0.6T_c$  the  $\rho(T, H)$  curves again become sharp. It is important to underline that the broadening occurs in the upper part of the  $\rho(T, H)$  curves, close to onset of the transition. No pronounced tails in the  $\rho(T, H)$  dependencies, which can be associated with the dishomogeneity of the samples or flux creep processes, have been ever observed.

The effect is analyzed within the continuous GL model with piecewise-constant coefficient functions,<sup>15</sup> which allows us to correctly analyze the nucleation points and to successfully fit the temperature dependences of the perpendicular  $H_{c2\perp}$  and parallel  $H_{c2\parallel}$  critical magnetic fields in our samples. As one of the possible explanations for the broadening of the  $\rho(T, H)$  curves in a temperature range close to  $T_c$  we consider the mechanism proposed by Fink for a superconducting homogeneous slab, which provides the nascent vortex chain in the center of the sample at fields

slightly less the  $H_{c2}$ .<sup>16</sup> In our case, as computations reveal, the vortex chain is also nascent in the center of the symmetry plane of the sample at  $H \leq H_{c2\parallel}$ . We demonstrate that the geometrical symmetry of the N/S multilayers leads to different results for the common action of the Lorentz and pinning forces on vortices.

Experiments were performed on Cu/Nb multilayers grown on Si(100) substrates at room temperature using a dual source magnetically enhanced dc triode sputtering system.<sup>17</sup> The high quality layered structure of samples with a negligibly small interfacial roughness ( $< 10 \text{ \AA}$ ) was confirmed by high and low angle x-ray diffraction measurements using a four axes Philips X'Pert MRD PRO diffractometer. dc transport measurements with a standard four probe technique were performed for both parallel and perpendicular magnetic field orientations. All the Cu/Nb multilayers have identical Cu ( $d_N$ ) and Nb ( $d_S$ ) thickness,  $d_N = d_S = 200 \text{ \AA}$ ,<sup>18</sup> but a different value of  $N_b$ . For all the samples Cu is the top and bottom layers. In general the sample indicated as  $MLN_b$  means, in fact, a number of Cu/Nb bilayers equal to  $N_b$ , plus a top Cu layer of the same thickness. The  $N_b$  values were changed from 5 to 12. Such a geometry gives the possibility to change the position of the symmetry plane of multilayer between the center of S layer (odd  $N_b$ ) and the center of N layer (even  $N_b$ ). Moreover, the pairs with  $N_b = 5$  and 6,  $N_b = 7$  and 8,  $N_b = 9$  and 10, and  $N_b = 11$  and 12 were each simultaneously prepared due to a specially designed shutter. The Nb properties were the same for each pair, as was checked by depositing single Nb films with  $d_S = 1300 \text{ \AA}$  on Si substrates situated on the positions used to create S- and N-type samples. The superconducting and normal properties of these Nb films were exactly the same ( $T_c = 8.85 \text{ K}$ , low temperature resistivity  $\rho_{10 \text{ K}} \approx 5 \mu\Omega \text{ cm}$ , and residual resistivity ratio  $\beta_{10} = \rho_{300 \text{ K}} / \rho_{10 \text{ K}} = 2.9$ ). The low temperature resistivity of the multilayers varies in the range  $7 \dots 9 \mu\Omega \text{ cm}$ ,  $T_c$  values were between 6.7 K for ML5 and 7.1 K for ML12, the transition widths at zero field  $\Delta T_c < 40 \text{ mK}$  (10–90% criterion with a bias current density of  $40 \text{ A/cm}^2$ ) and  $\beta_{10} = 1.7$ . The parallel coherence length  $\xi_{\parallel}(0)$ , extracted in the usual way from the  $H_{c2\parallel}(T)$  dependences at  $T \rightarrow T_c$ , was  $\approx 150 \text{ \AA}$  for S-type samples and  $\approx 135 \text{ \AA}$  for N-type samples. Based on the above experimental facts we believe that all our samples present identical Nb properties as well as the same interfaces between each layer. The only difference between the S- and N-type samples is their variable position of the symmetry plane.

We first show the experimental results regarding the different shape of the resistive transitions for S- and N-type samples in parallel magnetic field. In Fig. 1(a) the  $\rho(T, H)$  curves are shown for N-type samples at given  $H$  values. All the resistive transitions are sharp,  $\Delta T_c < 0.1 \text{ K}$ . This is the typical picture for N-type samples in the whole investigated temperature and magnetic field ranges. More intriguing is the  $\rho(T, H)$  behavior shown in Fig. 1(b) for S-type samples at given  $H$  values. In a wide temperature range ( $\sim 2 \text{ K}$ ) we *always* observed for *all* S-type samples a broadening of the transition in the *upper* part of resistive curve. The effect is less pronounced while increasing the  $N_b$  value. The  $\Delta T_c$  values for ML5 and ML7 samples become of the order of 0.5

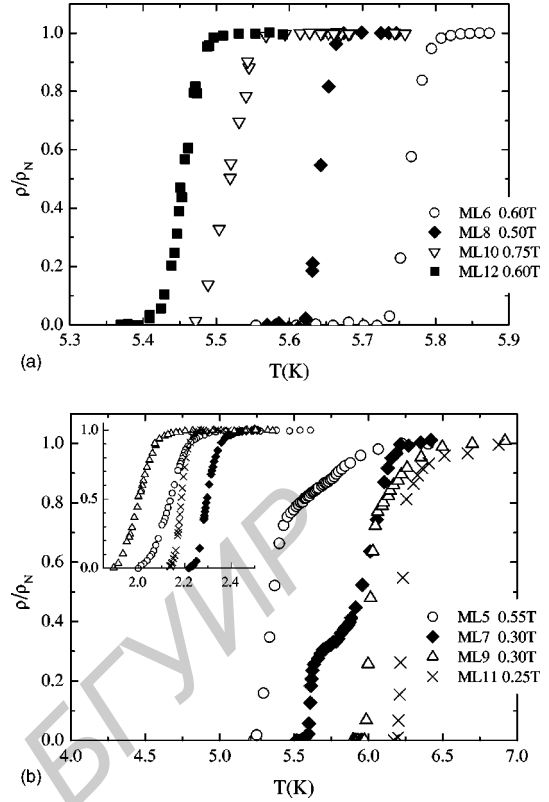


FIG. 1. (a)  $\rho(T)$  curves of N-type samples in parallel magnetic fields. (b) Examples of  $\rho(T)$  curves of S-type samples at parallel magnetic fields in the temperature range  $0.6 < T/T_c < 0.9$ . Inset: Examples of  $\rho(T)$  curves of S-type samples at parallel magnetic fields for temperatures  $T < 0.5T_c$ . Symbols are the same as for the main frame. Magnetic fields are 2.4 T for ML5, 2.2 T for ML7, 2.4 T for ML9, and 2.3 T for ML11.

K; for ML9 it is  $\approx 0.25 \text{ K}$  and for ML11 it is  $\approx 0.12 \text{ K}$ . Outside this temperature range the resistive curves are sharp again, and we measured  $\Delta T_c < 0.15 \text{ K}$  for all samples for fields larger than  $2T$  [inset to Fig. 1(b)]. The dynamic of this change is clearly seen in Fig. 2(a), where we plot the  $\rho(T, H)$  transitions for sample ML5. In Fig. 2(b) we show the  $H-T$  phase diagram for this sample. The  $H_{c2}$  values were extracted from the onset of the  $\rho(T, H)$  curves using a 90%  $\rho_N$  criterion. The solid and the dashed lines represent the result of the fitting procedure for  $H_{c2\parallel}(T)$  and  $H_{c2\perp}(T)$  dependencies, respectively, according to our model. In this figure we also present data related to the  $H_{c2\parallel}$  determination according to the 50%  $\rho_N$  criterion. All these results will be discussed later.

In the description of the superconducting properties of the even-odd multilayers, we rely upon the GL theory. We consider a system of coordinate with the  $XY$  plane parallel to the layer surface, coincident with the symmetry plane of the N/S structure, and the  $Z$  axis perpendicular to the layer surfaces. In the vicinity of  $H_{c2\parallel}$  the vector potential  $\mathbf{A}(\mathbf{r})$  is  $\mathbf{A}(\mathbf{r}) = (H_0 z, 0, 0)$ , where  $H_0$  is the external magnetic field. By separating the variables for the wave function in the  $XZ$  plane,  $\Psi(\mathbf{r}) = e^{ikx} \cdot \psi(z)$ , we get an equation for  $\psi(z)$ ,<sup>15,19</sup>

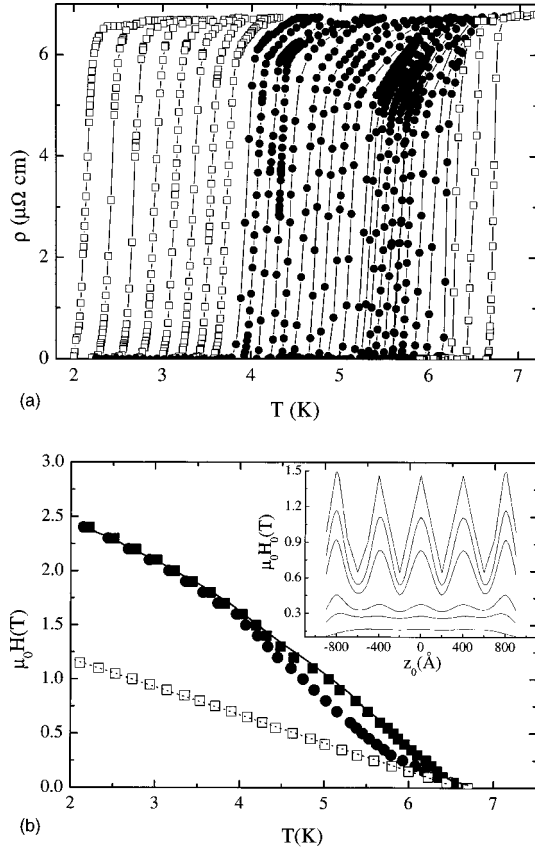


FIG. 2. (a)  $\rho(T)$  curves of sample ML5 in the parallel magnetic field. By closed symbols we marked the curves for which the broadening occurs ( $0.15 \text{ T} < \mu_0 H < 1.60 \text{ T}$ ). The magnetic fields change from 0 to 2.4 T. (b)  $H-T$  phase diagram for sample ML5. Open squares correspond to  $H_{c2\perp}(T)$ . Close squares (circles) correspond to  $H_{c2\parallel}(T)$  extracted by using the 90% (50%)  $\rho_N$  criterion, respectively. Drawn lines are model fits. Inset: The  $H_0$  distribution in sample ML5 at different temperatures (from up to down,  $T=4.3, 4.9, 5.3, 5.9, 6.1, \text{ and } 6.4 \text{ K}$ ).

$$(\partial_z^2 + \eta(z) - H_0^2 \cdot (z - z_0)^2) \psi(z) = 0, \quad (1)$$

where we have defined  $z_0 \equiv k/H_0$  and  $\eta$  is the step function.<sup>15</sup> The boundary conditions for the wave function  $\psi(z)$  are

$$\frac{\partial \psi}{\partial z}(L/2) = \frac{\partial \psi}{\partial z}(-L/2) = 0, \quad (2)$$

where  $L$  is the overall multilayer thickness. At each N/S interface Eq. (1) is accompanied by the condition<sup>1(a),20</sup>

$$\frac{1}{\psi_S} \frac{\partial \psi_S}{\partial z} \Big|_{\Gamma_i} = P \frac{1}{\psi_N} \frac{\partial \psi_N}{\partial z} \Big|_{\Gamma_i}, \quad (3)$$

where  $i = 1, 2, \dots, 2N_b$ ,  $P$  is the boundary transparent coefficient, and  $\psi_{S(N)}$  is the wave function in the S(N) layer. Conditions (2) and (3) at fixed temperature and for each value of  $z_0$  determine the eigenvalues problem  $H_0 = H_0(z_0)$  for Eq. (1) and the boundary conditions for the field  $H(r)|_{z=\pm L/2} = H_0$  give the equation for the parameter  $z_0$ :

$$\int_{-L/2}^{L/2} (z - z_0) \psi^2(z) dz = 0. \quad (4)$$

The maximum eigenvalue of  $H_0(z_0)$  is the upper critical field  $H_{c2\parallel}$ .

At the same time we can obtain the position of the superconducting phase nucleus, which is determined by the parameter  $z_0$ . Numerical calculation of  $H_0(z_0)$  dependence for sample ML5 [inset to Fig. 2(b)] reveals its oscillating character in the overall temperature range except in the region close to  $T_c$ . We found that the local maxima of the function  $H_0(z_0)$  belong to the centres of the S layers, while local minima fall in the centres of the N layers. Moreover, the highest local maxima correspond to the values  $z_0 \approx \pm(L/2 - d_N - d_S/2)$ . This means that the superconducting phase nucleus is formed in one of the two outer superconducting layers. For sufficiently low temperatures the difference among the local maxima of  $H_0(z_0)$  becomes smaller and the superconducting nucleus is confined in each S layer with almost equal probability. This means that for low temperatures the well known<sup>1,2,5</sup> two-dimensional (2D) behavior of the superconducting phase of the infinite superconducting superlattice takes place. Considerations for the case of high temperatures could be done on the base of the works for superconducting homogeneous slab.<sup>16,21</sup> For  $T \approx T_c$  the GL wave function is delocalized over the whole sample and becomes symmetrical with respect to  $z=0$ . As a result of these considerations we obtain a theoretical description of the  $H_{c2\parallel}(T)$ , which well describes the whole experimental curve. This result for sample ML5 is shown in Fig. 2(b) by the solid line. For sample ML5 we found the following reasonable fit parameters:  $P=0.34$ , and the correlation lengths in the superconducting (normal) layer of  $\xi_{S(N)} = 123$  and  $140 \text{ \AA}$  respectively. More details about the  $H_{c2}$  calculations according to the proposed model are reported elsewhere.<sup>15</sup> The successful fitting procedure was available for both the  $H_{c2\perp}(T)$  and  $H_{c2\parallel}(T)$  dependencies with the same fit parameters *only* for the  $H_{c2\parallel}$  values obtained at the onset of the  $\rho(T, H)$  curves. Obviously, when resistive curves are sharp (as in the case of perpendicular field orientation) there is no difference between the  $H_{c2}$  values obtained according to different criteria. Given the definition of  $H_{c2}$  as the field of superconducting phase nucleation, it seems reasonable to choose the 90%  $\rho_N$  criterion for its determination.

Now we will focus on the dependence of the vortex lattice nascent process at  $H \leq H_{c2}$  on the  $\rho(T, H)$  curves. At low temperatures, when the superconducting nucleus could be found in each of S layers with almost the same probability, a rather stable vortex lattice is formed at  $H_0$ , slightly less than  $H_{c2\parallel}(T)$ . The perturbation of the lattice due to feeble bias current is smaller with respect to the interface pinning force. The  $\rho(T)$  curve is sharp both for S- and N-type samples. This scenario is relatively trivial. The physical picture becomes complicated when the temperature increases towards the critical  $T_c$  value, namely, at temperatures corresponding to the observed spread of the resistive characteristics for S-type samples. At this temperature the double degeneracy of  $H_{c2\parallel}$  occurs [see the inset to Fig. 2(b)]. This leads to another scenario of the vortex lattice rising at  $H \leq H_{c2}$ .



In order to construct the first order perturbation theory wave function,<sup>19</sup> describing the superconducting state in the vicinity of  $H_{c2}$ , the ground state wave function must be written as

$$\Psi^{(0)}(\mathbf{r}) = c_1 e^{ikx} \cdot \psi(z) + c_2 e^{-ikx} \cdot \psi(-z), \quad (5)$$

with the unknown coefficients  $c_1$  and  $c_2$ . One of the results of the first order perturbation theory standard calculations is the equality  $c_1 = c_2$ . It follows that wave function (5) has a chain of zeroes along the  $OX$  axis with the period  $\Delta x = \pi/k$ . This means the formation of a one-dimensional (not two-dimensional, as at low temperatures) vortex lattice in the symmetry plane  $XOY$  of the multilayer. This vortex chain does not possess the stability of the usual vortex lattice with respect to the external perturbations. That is, resistive measurements imply a perturbation of the superconducting state due to the bias current (it flows along the  $OX$  axis), so the Lorentz force acts on vortices in the  $OZ$  direction. In addition, vortices are in the pinning potential field, which is created by the inhomogeneous periodical structure of the sample. The result of the common action of the pinning and Lorentz forces on the vortex chain, as our calculations reveal, depends on the symmetry type of the samples. The pinning force  $F_p$ , obtained according to the procedure elaborated in Ref. 7, may be expressed as

$$F_p = \mp \sum_{l=-[N_b/2]}^{[(N_b-1)/2]} \left( \frac{\xi_S^2(T)}{\xi_N^2(T)} + 1 \right) \left[ f^2 \left( \frac{d_{S,N}}{2} - z_v + l(d_S + d_N) \right) - f^2 \left( -\frac{d_{S,N}}{2} - z_v - l(d_S + d_N) \right) \right] + \frac{\xi_S^2(T)}{\xi_N^2(T)} \left[ f^2 \left( \frac{L}{2} - z_v \right) - f^2 \left( -\frac{L}{2} - z_v \right) \right], \quad (6)$$

where the sign  $- (+)$  before the sum corresponds to S- and N-type samples, respectively and  $z_v$  is the  $z$ -coordinate of the vortex chain. It can be seen from Eq. (6), that in both cases due to oddness of the function  $f^2(z) \equiv \langle |\Psi^{(0)}(x,z)|^2 \rangle_x$  the point  $z_v = 0$  is the equilibrium point of the vortex chain. For N-type samples, when the vortex chain is situated in the center of the N layer, this equilibrium position is stable. The bias current flows through the superconducting parts of the sample, dissipative processes are absent and the resistive transition is sharp [Fig. 1(a)]. For S-type multilayers, vortices, which are nascent in the central S layer, are in a metastable state. In this way finite size effects enter through the stability of the nascent vortices. The  $\rho(T,H)$  transitions become broader when it is less favorable to lock in vortex chain. Finally, the less pronounced broadening, observed for sample ML11 in Fig. 1(b), could be due to the less influence of the surface effects with increasing  $N_b$  value on the discussed processes. This will be the subject of future studies.

In summary, we have observed the broadening of the resistive characteristics above the temperature of the 2D-3D dimensional crossover in Cu/Nb multilayers with the symmetry plane in the center of the S layer. When the symmetry plane is in the center of the N layer, the transition curves are always sharp. We analyzed the nucleation points of the superconducting phase at different temperatures in order to build the  $H-T$  phase diagram, and we found that the agreement between the model and experiment can be reached only when the  $H_{c2}$  values are determined at the onset of the resistive transitions. This gives us a reason to explain qualitatively the observed broadening of the  $\rho(T,H)$  curves as the result of the influence of the finite size effects on the stability of the nascent vortices in the symmetry plane of the N/S multilayers. The precise configuration of the vortex lattice in such multilayers could be controlled using modern imaging methods.<sup>22,23</sup>

<sup>1</sup>For reviews of early research see (a) B.Y. Jin and J.B. Ketterson, *Adv. Phys.* **38**, 189 (1989); (b) A.N. Lykov, *ibid.* **42**, 263 (1993).  
<sup>2</sup>S. Takahashi and M. Tachiki, *Phys. Rev. B* **33**, 4620 (1986); **34**, 3162 (1986).  
<sup>3</sup>R.T.W. Koperdraad and A. Lodder, *Phys. Rev. B* **54**, 515 (1996).  
<sup>4</sup>Ya.V. Fominov and M.V. Feigel'man, *Phys. Rev. B* **63**, 094518 (2001).  
<sup>5</sup>R.A. Klemm, A. Luther, and M.R. Beasley, *Phys. Rev. B* **12**, 877 (1975).  
<sup>6</sup>E.H. Brandt, *Rep. Prog. Phys.* **58**, 1465 (1995).  
<sup>7</sup>V.N. Kushnir, S.L. Prischepa, C. Attanasio, and L. Maritato, *Phys. Rev. B* **63**, 092503 (2001).  
<sup>8</sup>C. Ciuhu and A. Lodder, *Superlattices Microstruct.* **30**, 95 (2001).  
<sup>9</sup>C. Ciuhu and A. Lodder, *Phys. Rev. B* **64**, 224526 (2001).  
<sup>10</sup>J. Aarts, *Phys. Rev. B* **56**, 8432 (1997).  
<sup>11</sup>I.K. Schuller, *Phys. Rev. Lett.* **44**, 1597 (1980).  
<sup>12</sup>V.L. Ginzburg and L.D. Landau, *Zh. Eksp. Teor. Fiz.* **20**, 1064 (1950).  
<sup>13</sup>T. Kogama, N. Takezawa, Y. Naruse, and M. Tachiki, *Physica C*

**194**, 20 (1992).

<sup>14</sup>C.S.L. Chun, G.-G. Zheng, J.L. Vicent, and I.K. Schuller, *Phys. Rev. B* **29**, 4915 (1984).  
<sup>15</sup>V.N. Kushnir, A.Y. Petrov, and S.L. Prischepa, *Low Temp. Phys.* **25**, 948 (1999).  
<sup>16</sup>H.J. Fink, *Phys. Rev.* **177**, 732 (1969).  
<sup>17</sup>L.V. Mercaldo, C. Attanasio, C. Coccorese, L. Maritato, S.L. Prischepa, and M. Salvato, *Phys. Rev. B* **53**, 14040 (1996).  
<sup>18</sup>For these  $d_N$  surface superconductivity could not yet be ignored (Ref. 8).  
<sup>19</sup>A.A. Abrikosov, *Fundamentals of the Theory of Metals* (Nauka, Moscow, 1987).  
<sup>20</sup>P.G. de Gennes, *Rev. Mod. Phys.* **36**, 225 (1964).  
<sup>21</sup>D. Saint-James and P.G. de Gennes, *Phys. Lett.* **7**, 306 (1963).  
<sup>22</sup>A. Tonomura, H. Kasai, O. Kamimura, T. Matsuda, K. Harada, Y. Nakayama, J. Shimoyama, K. Kishio, T. Hanaguri, K. Kitazawa, M. Sasase, and S. Okayasu, *Nature (London)* **412**, 620 (2001).  
<sup>23</sup>M.J. Van Bael, M. Lange, S. Raedts, V.V. Moshchalkov, A.N. Grigorenko, and S.J. Bending, *Phys. Rev. B* **68**, 014509 (2003).